

# Gradient of Birefringence: A New Direction for Gradient Optics

L. Nadareishvili,<sup>1</sup> S. Gvatua,<sup>1</sup> I. Blagidze,<sup>1</sup> G. Zaikov<sup>2</sup>

<sup>1</sup>*Institute of Cybernetics, Georgian Academy of Sciences, 5, S. Euli St., 380081 Tbilisi, Russia*

<sup>2</sup>*N. M. Emanuel Institute of Biochemical Physics, Russian Academy of Sciences, 4, Kosigin Str., 117334 Moscow, Russia*

Received 10 June 2002; accepted 24 February 2002

**ABSTRACT:** The fabrication of a new type of polymeric optical element with specified properties with a given axial gradient of birefringence (GB) is described. The estimation of some technological spaces of GB element fabrication is given. For the fabrication of GB elements, an inhomogeneous mechanical field with a given heterogeneity was used. GB elements on poly(vinyl spirit) and polyethylenetereph-

thalate thin films bases were created, and their properties were investigated. The maximal value of the implemented birefringence was  $1.4 \times 10^{-2}$ . © 2003 Wiley Periodicals, Inc. *J Appl Polym Sci* 91: 489–493, 2004

**Key words:** polymers; films; drawing; orientation; optics

## INTRODUCTION

The worldwide general practice in gradient optics has been to focus attention only on the refractive index gradient. However, materials with gradients of other optical properties are also of interest and, in particular, those with a gradient of birefringence (GB). Optical polymeric films with a linear GB can be used in polarimetries for various applications, including equalizers for the measurement of birefringence values and the study of the character of birefringence distribution.

Earlier, we, as it seemed for the first time, described the reception of polymeric films with a given axial GB.<sup>1–3</sup> We suggested that such a film should be called a GB element or GB material.

The successful creation of GB elements, the investigation of their properties, and the determination of the fields of their application require a broadening of the notion of gradient optics, with a subdivision into two groups: gradient refractive index optics, or the optics of materials with a refraction gradient, and GB optics, the optics of materials with a GB.

In this article, the technological aspects of creation of the GB elements and the results of an investigation of their properties are reported.

It is common knowledge the deformation of polymers above the glass-transition point is accompanied by the uncoiling of flexible chains of macromolecules and the orientation of their segments in the stretch direction. The sample thus obtains the symmetry of a

one-axis crystal the optical axis, that coincides with the stretching direction. The orientation of optically anisotropic molecular chains is the reason for the occurrence of birefringence in the polymer, which is a function of the relative stretch deformation of the sample:

$$\Delta n = n_1 - n_2 = \gamma \eta \quad (1)$$

where  $\Delta n$  is birefringence;  $n_1$  and  $n_2$  are the refractive indices of the singular and ordinary rays, respectively;  $\gamma$  is the optical deformation coefficient; and  $\eta$  is the relation of elongation to the initial sample length.

With the one-axis stretching of a rectangular-shaped polymer film, elongation along the width of the film is practically the same. That is why the orientation degree and, consequently, the birefringence in the direction perpendicular to the stretching are the same. Strictly speaking, elongation along the sample surface is different even under conditions of homogeneous stretching; that is, if a “neck” does not occur. Elongation increases on both sides from the central part of the sample in the direction of their free (unfixed) edges, which shows as a narrowing of the sample, which in turn, increases from the fixed ends of the sample to its center in the stretch direction. The relative values of narrowing and their distribution in the stretch direction depend on relation of the ratio of rectangle side lengths and the deformation mode (rate, relative elongation, temperature, etc.). Nevertheless, this difference in the values of elongation can be neglected because it is insignificant for the formation of a practical GB. If a trapezium-shaped (equilateral nonequilateral) sample is stretched, that is, when clips 1 and 3 are disposed on nonparallel lines but at some chosen angle (Fig. 1), the relative elongation over height  $h$  will be different. It

Correspondence to: G. E. Zaikov.

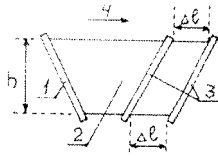


**Figure 1** Scheme of sample stretching without an elongation gradient.

will increase from the longer side of the trapezium to the smaller one. This, according to eq. (1), provides for the GB growth in the same direction. Clearly, if at the along (free) edge of sample 2 (at the longer side of the trapezium), elongation is zero, the range of GB will be maximal.

## RESULTS AND DISCUSSION

Described next is a device for obtaining a GB element. It allows for the formation of an inhomogeneous mechanical field with the required degree of inhomogeneity, the application of which to the sample forms the given axial gradient of elongation (the given gradient of orientation degree of molecular/overmolecular structure) and, consequently, the given axial GB.

The principal features of the device are shown in Figure 2. Sample 8 (a film, a plane), trapezium-shaped and of height  $h$ , is fixed by two clips, 3 and 6, with nonparallel chamfered rims. To demonstrate the character of elongation distribution, a grid can be applied to sample 8. Clips 3 and 6 are rotated in opposite directions around parallel axes 4 and 5 by an electric motor with reducing gear 1 and gearwheels 2 and 7. As clips 3 and 5 rotate, their rims, in fact, are moving along the surfaces of round cones, the generatrices of which are disposed at angles of  $\varphi_1$  and  $\varphi_2$  to the heights of the cones, coincident with rotation axes 4 and 5 in space. Clips 3 and 6 (clip rims) can be separately set at different angles to rotation axes 4 and 5. Therefore, different variants are available:  $\varphi_1 \geq \varphi_2$  or  $\varphi_1 > 0$  and  $\varphi_2 = 0$ . The points of intersection of the rims of clips 3 and 6 with rotation axes 4 and 5 are static (immovable). The distance between them equals the length of the greater side of the trapezium, the maximal length of the initial sample 8, and remains constant during elongation:  $l_{\max} = l(x = 0; 0^\circ \leq \alpha \leq 90^\circ) = \text{constant}$ , where  $\alpha$  is the rotary angle of clips 3 and 6, whereas movement from the longer side toward the smaller side of the trapezium, that is, from  $h = 0$  to  $h = h_{\max}$  the absolute elongation increases.

As shown next, a change in the sample appearance on elongation is governed by complicated rules. If the process of deformation is idealized and we assume conditionally that a change in distances between the rims of clips 3 and 6 (Fig. 2) accurately correspond to

the appearance and overall size of the sample, the following suggestions can be made:

- As clips 3 and 6 are rotated in the range  $0^\circ \leq \alpha \leq 90^\circ$ , both longitudinal and transverse elongation occur, the latter reducing the degree of anisotropy.
- It can be shown that for the case  $\varphi_1 = \varphi_2 = \varphi$ , the length and width increments are, respectively:

$$\Delta l = 2h \times \text{tg} \varphi (1 - \cos \alpha) \quad (2)$$

$$\Delta h = h_{\max} (\sqrt{1 - \sin^2 \varphi \times \text{tg}^2 \varphi} - 1) \quad (3)$$

- Conditions under which the inequality

$$\Delta h < \Delta l \quad (4)$$

is fulfilled must be estimated as the criterion for providing dominant orientation and, consequently, advisability of application of the method. It can be easily shown that eq. (4) is equivalent of the inequality  $\cos \alpha < 1 - \Delta h / 2R$  (where  $R$  is the base radius of the imaginary cones along the surface of which clips 3 and 6 are moved and  $\Delta h < R$ ). Therefore, it follows that eq. (4) is true at any value in the range  $0-90^\circ$ . Clearly, if  $\alpha > 90^\circ$ ,  $\Delta h$  decreases, and the sample must be narrowed, whereas  $\Delta l$  increases continuously.

- If  $\varphi_1 = \varphi_2$ , as clips are rotated by  $90^\circ$ , the length of sample 8 remains the same over the whole width  $x$  and equals the maximal initial length:

$$l(0 \leq x \leq h; \alpha = 90^\circ) = l(x = 0; 0^\circ \leq \alpha \leq 90^\circ)$$

- The sample attains a rectangle shape; its width equals the length of the generatrix of the imaginary cones on the surface of which clips 3 and 6 are moving.

Clip rims can be not only linear but may possess a more complicated, almost arbitrary shape when  $\varphi$  is

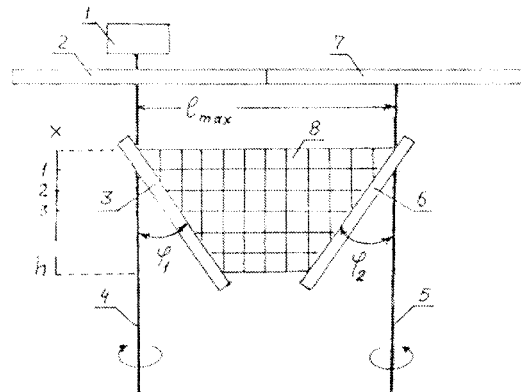


**Figure 2** Scheme of a device for sample stretching with an elongation gradient.

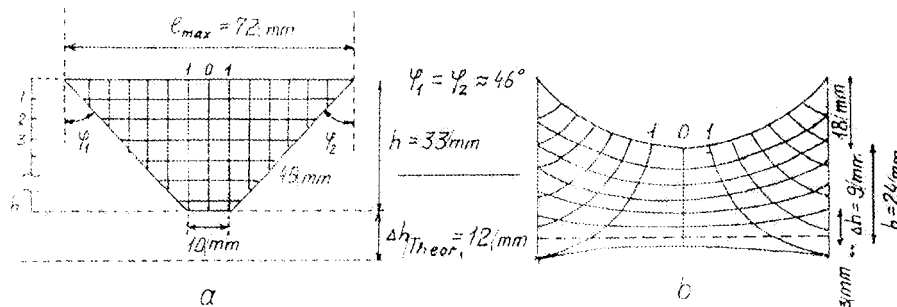


Figure 3 Topographic image of deformation distribution in the PVS film at stretching with an elongation gradient.

different for separate parts or is changing continuously. For such cases, eq. (2) can be reduced to another form when one takes into account that  $r = htg\varphi$ , where  $r$  is the clip rim distance from the rotation axis in the stretch direction on the value of  $h$  chosen.

In the device described, the maximal rotation of clips 3 and 6 is  $\alpha_{max} = 90^\circ$ . As  $\alpha > 90^\circ$ , sample 8 will be applied to the rims of clips 3 and 6, which lead to the break. Therefore, constructions were suggested in which  $\alpha_{max} = 180^\circ$ .<sup>4</sup>

The transparent polymers polyvinyl spirit (PVS) and polyethyleneterephthalate (PET) were taken as the objects of investigation. PVS films were produced with well-known methods, and PET films were factory manufactured.<sup>5</sup>

For the described installation of axial GB elements, isotropic amorphous films of PVS and PET with thicknesses of 80–120  $\mu\text{m}$  and 190  $\mu\text{m}$ , respectively, were received. Initial samples, as rectangular trapezes with big (72 mm) and small (10 mm), were lengths deformed in water at 20°C (PVS) and in air at 80°C (PVS and PET). The angular spaces of clips 3 and 6 are a rotation of  $\varphi = 46^\circ$  was 0.0785  $\text{s}^{-1}$ ; the corner of the turn of clips 3 and 6 was  $\alpha = 90^\circ$ .

As an example, in Figure 3 is shown a typical scheme of the sample (PVS film) with an applied grid before and after elongation (rotation angle of clips  $\alpha = 90^\circ$ ). A complex connection between the features of the superposed inhomogeneous mechanical field and the topographical picture of deformation distribution was observed. The sample was elongated inhomogeneously. The area of dominant deformation, localized in the sample center in its upper part, gradually spread down the whole width in the sample. At maximal (theoretical) elongation of the lower rim of the sample, equal to 620%, longitudinal elongation was  $\Delta h = 8.5\text{--}9\text{ mm}$  (~75% from theoretical one). Gradient deformation provided for a clearly expressed dominant narrowing of the sample in the upper part. The initial horizontal rim of the sample corresponding to  $h = 0$  was elongated by about 10%. The shortest width of the sample was 24 mm. The sample material shifted downward, and the noncurved horizontal line repre-

sented a somewhat center of gravity of the narrowing [dotted line in Fig. 3(b)], which in the case of the parallel clips applied was disposed in the central zone of the sample and, in this case, was strongly shifted to the side of the most elongated part.

Research on the polarizing characteristic of the gradient orientation of the polymeric films was made with the help of a Berek's equalizer and a MIN-8 polarizing microscope and also a laboratory experimental installation, whose optical circuit is shown in Figure 4.

The linear polarized radiation of an LG-201 type 1 He-Ne laser with a wavelength  $\lambda = 632,8\text{ nm}$ , and the diameter of a beam of  $\phi = 1\text{ mm}$  fell perpendicularly on researched sample 2, fixed in a module frame that had the opportunity to move in a horizontal plane with uniform speed with the help of a type RD-09 low turnaround electromotor 3. The frame with sample 2 was also placed in a vertical plane at a required level concerning the central axis of the GB element as the analyzer in the Roshon prism 4. In the radiation, the passing prism 4 fell on the photodiode 5 FD-01k type and was recorded on a one-coordinate recorder KSP-4 recorder. The plane in which the electric vector of an oscillation linear polarized laser radiation laid, was fixed under a corner  $45^\circ$  to an optical axis of the GB element with the help of the Roshon prism 4 (the exactitude of angular fixation was  $\pm 30'$ ). We recorded the dependence diagram value of birefringence along the central axis of the GB element from the width  $h$  at the crossed position of the electric vector of a laser beam and the analyzer 4 at their parallel position.

It is known<sup>6</sup> that the intensity of monochromatic light radiation, passed through the previously de-

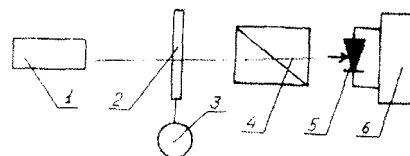
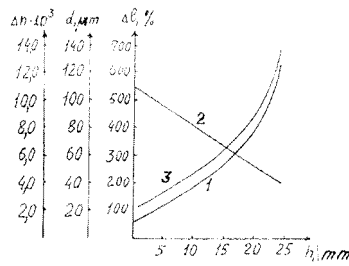


Figure 4 Optical scheme of installation for birefringence measurement.



**Figure 5** Distribution of elongation (curve 1), thickness (curve 2), and birefringence (curve 3) by width of the GB element from PVS deformed in water at 20°C.

scribed installation at the crossed position of an oscillation plane of a beam 1 electric vector and analyzer 4 [under the condition that the polarization plane of the laser beam (E vector) makes a corner of 45° with an optical axis of the researched polymeric sample] can be determined by expression:

$$I_{\perp} = I_0 \sin^2[(\pi/\lambda) \times \Delta n \times d] \quad (5)$$

At the parallel position of the appropriate polarization planes

$$I_{\parallel} = I_0 \cos^2[(\pi/\lambda) \times \Delta n \times d] \quad (6)$$

where  $I_0$  is intensity of the laser beam falling on the researched sample,  $\lambda$  is length of the laser radiation wave,  $d$  is the thickness of the researched sample, and  $\Delta n$  is the value of birefringence. When we divide the appropriate left and right parts of eqs. (5) and (6) against each other, we get

$$\text{tg}^2[(\pi/\lambda) \times \Delta n \times d] = I_{\perp}/I_{\parallel} \quad (7)$$

Equation (7) allows us to calculate the value of birefringence from the dependence diagrams from the width.

Figure 5 shows the quantitative characteristics of the GB element from PVS produced by this method.

Curve 1 (Fig. 5) displays the distribution of the longitudinal elongation by PVS width deformed in an inhomogeneous mechanical field. Countdowns were made for the most deformed part of the film, marked by 1-1 in Fig. 3(b). It is clear from the figure that a jump of elongation existed in the sample, changed by a decimal degree. Under special conditions, the elongation jump could be increased by 2–3 decimal degrees.

Curve 2 (Fig. 5) shows the dependence of the sample thickness on its width. The countdowns were taken by the zero line located in the middle of the sample [Figure 3(b)]. As expected, the sample thickness was reduced as the longitudinal elongation increased.

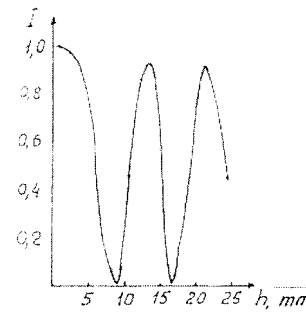


**Figure 6** Dependence of relative light intensity passing through a PVS film width of the GB element.

Finally, curve 3 (Fig. 5) shows the distribution of birefringence over the width (on the zero line) of the same sample. Measurements were performed with the help of a Berek equalizer. Figure 5 shows that the sample possessed a clearly displayed axial GB in complete concordance with the character of elongation (curve 1) and thickness (curve 2).

Figure 6 shows the dependence of the relative light intensity passing through the same sample from PVS with a GB ( $\lambda = 0.63 \mu\text{m}$ , junction Nicols). Countdowns were made by the same zero line [Fig. 3(b)]. The figure shows that the light intensity passing through the PVS film was modulated depending on the values of width coordinate with quite good correspondence to eq. (5).

In Figure 7 are submitted values of birefringence [ $\Delta n = f(h)$ ] calculated from eq. (7) with the help of experimental diagrams  $I_{\perp} = f(h)$  and  $I_{\parallel} = f(h)$ , appropriate to eqs. (5) and (6). Apparently, the character of birefringence distribution on the width of PVS film

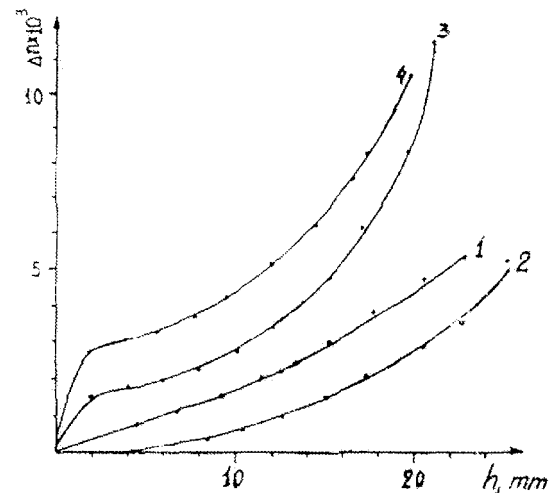


**Figure 7** Distribution of birefringence on width  $h$  of GB-elements: (1) PET [thickness = 190  $\mu\text{m}$ , deformation temperature ( $t$ ) = 80°C, and  $\alpha = 80^\circ$ ], (2) PET [thickness = 200  $\mu\text{m}$ ,  $t = 80^\circ\text{C}$ , and  $\alpha = 60^\circ$ ], (3) PVS [thickness = 190  $\mu\text{m}$ ,  $t = 80^\circ\text{C}$ , and  $\alpha = 90^\circ$ ], and (4) PVS [thickness = 110  $\mu\text{m}$ ,  $t = 80^\circ\text{C}$ , and  $\alpha = 90^\circ$ ].

was similar to the results received with the Berek equalizer (Fig. 5). For PET films the dependence  $\Delta n = f(h)$  was closer to linear in comparison with PVS films. However, for PVS, a higher birefringence value was realized, especially for the samples deformed in water. The increase in birefringence was also precisely traced in the process of the lengthening increase and thickness reduction of the films.

Hence, for the strict regulation of the values range and the structure of birefringence distribution, careful research is needed on how such factors influence the nature of a polymer and the mode of deformation (temperature, speed of deformation, distribution of relative lengthening on the width of a sample, environment, and singularity of a nonuniform mechanical field).

### CONCLUSIONS

The importing of new parameter in optics, GB, formed the basis for a new direction for formation gradient optics: GB optics.

GB elements were created in an inhomogeneous mechanical field with a given heterogeneity.

The constructions for inhomogeneous mechanical field formation with the given heterogeneity were considered. The birefringence distributions in polymeric films were researched.

GB elements based on transparent thin PVS and PET films were made.

We showed experimentally that the manufacturing condition variation of GB elements could be operated with the structure of birefringence distribution and its range.

The experimental results of the investigation of polymeric GB elements obtained in this study allow us to state that they will find wide application in optical instrument-making in the form of polarized equalizers, polarimeters, and other polarized elements as well as in different fields of science and technology, such as integral optics, optical communication systems, multilayer polymeric birefringent mirrors, and filters.<sup>7</sup>

### References

1. Nadareishvili, L.; Gvatua, S.; Lekishvili, N.; Gvatua, N.; Japaridze, K. Programme and Book of Abstracts, International Conference of Polymer Characterization, POLYCHAR-8, Denton, TX, 11–14 Jan 2000; p 60.
2. Nadareishvili, L.; Gvatua, S. The Collection of the International Conference Works "Applied Optics—2000," St. Petersburg, Russia, 16 Oct 2000; Vol. 1, p 34.
3. Nadareishvili, L. GEN (Georgian Eng News) 2001, No. 2, 73.
4. Nadareishvili, L.; et al. Pat. Appl. 3523.
5. (a) Encyclopedia of Polymers: Sovetskaia, M., Ed.; 1974; Vol. 2, p 787; 1977; Vol. 3, p 112. (b)
6. Ilin, R.; Fedorov, G.; Fedin, L. Mech Eng 1966, 202.
7. Weber, M. F.; Stover, C. A.; Gilbert, L. R.; Nevitt, T. J.; Ouder Kirk, A. J. Science 2000, 287, 2451.